

# Triple Fluorescence of Substituted Benzanilides in Solution and in Solid States

S. Lucht,<sup>1</sup> J. Stumpe,<sup>2</sup> and M. Rutloh<sup>2</sup>

Received October 27, 1997; accepted May 14, 1998

The competitive triple fluorescence of benzanilide is studied by steady-state fluorescence investigations in dependence on the solvent polarity and the para-substitution of the aniline core as well as by comparison with the fluorescence behavior of 4-methoxy-*N*-methylbenzanilide. The normal fluorescence of benzanilide  $S_1(\text{LE}) \rightarrow S_0$  appears at  $\lambda_{\text{max}} = 345$  nm, whereas a superposition of proton transfer (PT) fluorescence  $S_1'(\text{PT}) \rightarrow S_0'(\text{PT})$  and intramolecular charge transfer (ICT) fluorescence  $S_1''(\text{ICT}) \rightarrow S_0(\text{FC})$  is responsible for the long-wavelength fluorescence in the 500-nm region. Different possibilities for the formation of the PT and ICT states are discussed. Investigations of the fluorescence behavior of benzanilides both in solution and as crystals in dependence on the para-substitution of the benzanilide moiety support the PT/ICT model.

**KEY WORDS:** Benzanilide; fluorescence; proton transfer; intramolecular charge transfer; solid-state fluorescence.

## INTRODUCTION

Although there exist several investigations concerning the photophysical behavior of benzanilide in solution, the interpretation of the deactivation mechanisms is not satisfactory.

The fluorescence spectrum of benzanilide in solution consists of a short-wavelength band whose maximum is at  $\lambda_{\text{max}} = 345$  nm and a large Stokes-shifted fluorescence in the wavelength region of 480 to 520 nm. The short-wavelength band is interpreted as the normal fluorescence of benzanilide  $F_1$  [ $S_1(\text{LE}) \rightarrow S_0$ ] [1]. Because of the large Stokes shift of the long-wavelength fluorescence O'Connell and Delmauro [2] conclude that changes of the geometry in the excited state are responsible for this fluorescence band. On the basis of steady-state and time-resolved fluorescence measurements of

several aromatic amides Azumaya *et al.* [3] interpret this long-wavelength band as a fluorescence from an intramolecular charge transfer state characterized by twisting of the excited molecule about the C–N bond (TICT fluorescence). On the other hand Heldt and Kasha [4–7] regard the long-wavelength fluorescence band as an overlapping of proton transfer (PT) fluorescence  $F_2$  [ $S_1'(\text{PT}) \rightarrow S_0'(\text{PT})$ ] and TICT fluorescence  $F_3$  [ $S_1''(\text{TICT}) \rightarrow S_0(\text{FC})$ ].

The TICT model was developed by Grabowski *et al.* [8] due to the discovery of the dual fluorescence of *p*-dimethylaminobenzonitrile by Lippert *et al.* [9]. The TICT state is formed by full or nearly full electron transfer between donor and acceptor group, which are twisted against each other by 90° [10]. While the PT fluorescence is preferably observed in aprotic solvents, the TICT state can be stabilized by increasing the environmental polarity.

An alternative model for the interpretation of the dual fluorescence was introduced by Zachariasse *et al.* [11,12]. It is based on a solvent-induced two-level coupling with an amino nitrogen inversion as the promoting

<sup>1</sup>Institute of Experimental Physics and Physical Didactic, University of Potsdam, Am Neuen Palais 10, 14469 Potsdam, Germany.

<sup>2</sup>Department of Chemistry, Humboldt University, Erieseering 42, 10319 Berlin, Germany.

mode. It is assumed that the amino nitrogen inversion results in a change in the configuration of the amino nitrogen group from pyramidal in the ground state to planar in the intramolecular charge transfer state (ICT).

The interest in investigations of the deactivation behavior of benzanilides results from their application as components for a variety of polymers, particularly liquid crystalline main-chain polymers. These aramides show excellent mechanical properties such as high tensile strength and good thermal and chemical stability resulting from the rigid rod-like shape of the benzanilides, the anisotropic intermolecular interactions, and their capability to form hydrogen bonds. The benzanilide group is also an interesting component for liquid crystalline side-group polymers, causing an increase in mesophase ranges and clearing points. These polymers are interesting materials for applications in optical data storage and nonlinear optics.

The aim of the study is to characterize the deactivation processes of benzanilide in dependence on solvent polarity, by variation of the substitution and by comparison of the fluorescence in solution and in solid states. The results of the fluorescence measurements are supplemented by further spectroscopic methods. More information about the micromorphology of polymers in the solid states and mesophases is expected from detailed fluorescence investigations.

## EXPERIMENTAL

The chemical structure of the investigated benzanilides is presented in Fig. 1 and Table I. The structure of the chromophores has been modified by donor and acceptor substitution in the para-position of the anilino aromatic ring and by a methyl group at the nitrogen atom.

Figure 2 demonstrates the structure of the investigated polymethacrylate with cyano substituted benzanilide side groups, which are coupled with the main chain by an ethylene spacer. The homopolymer **P5** was synthesized by radical polymerization of **M5**. **P5** is an amorphous polymer with a glass transition temperature of 130°C [13].

Fluorescence investigations of the solutions were carried out with an LS50 spectrometer (Perkin Elmer). The benzanilide monomers as well as the polymers were excited at a wavelength of  $\lambda_{\text{ex}} = 280$  nm and a slit width of 6 nm.

The following solvents (Merck) were used for the investigations: pentane, hexane, heptane, cyclohexane, 1,4-dioxane, toluene, dibutyl ether, diethyl ether, acetic acid, ethyl acetate, tetrahydrofuran, dichloromethane,

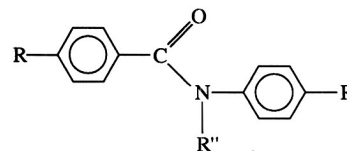


Fig. 1. Chemical structure of the benzanilides.

dichloroethane, and ethanol. Dibutyl ether, acetic acid, and ethyl acetate were purified for the analysis; the other solvents used were of Uvasol quality. In spite of the high degree of purity, some of the solvents (toluene, dibutyl ether, cyclohexane) exhibit intensive fluorescence upon excitation at 280 nm, which overlaps the normal fluorescence of benzanilide, especially in low concentrated solutions. For these solvents the normal fluorescence of benzanilide cannot be separated or is observable only in high concentrated solutions.

The solid substance emission spectra were recorded on a DILOR XY multichannel spectrometer coupled with a research-grade microscope. The equipment allows measurements with small amounts of substance where the observed region is about 5  $\mu\text{m}$  in diameter. Corresponding to the investigations in solution the excitation of the solid substances should be optimal with nearly 280 nm. But both available excitation light sources (argon ion laser with lines at 351.1 and 363.8 nm and xenon arc lamp with a double monochromator) allow excitation only in the long-wavelength region of the absorption spectrum of the benzanilides. But a comparison investigation of a spin-coated film of **P5** with the LS50 shows the same fluorescence behavior for excitation with both 280 and 350 nm. Moreover, using the DILOR spectrometer, signals can be detected only above 380 nm.

FTIR investigations were done with a FTIR2000 (Perkin Elmer). The x-ray investigations were carried out with a STOE  $\theta$ - $\theta$  diffractometer.

As the irradiation source for the photochemical investigations, a HBO lamp with an electrical power of 100 W was used. The sample was irradiated with a wavelength of  $(254 \pm 10)$  nm.

The absorption spectra were recorded with a LAMBDA2 (Perkin Elmer).

## RESULTS

### Investigations of the Photochemical Behavior of Benzanilide

It is known that benzanilides as well as other aromatic amides and esters undergo the photo-Fries reac-

Table I. Structure and Properties of the Investigated Benzanilides

	R	R'	R''	F (°C) <sup>a</sup>	$\lambda_{\max}$ (nm) <sup>b</sup>
M1	H	H	H	164	266
M2	CH <sub>3</sub> O	H	CH <sub>3</sub>	66–70	270 <sup>c</sup>
M3	CH <sub>2</sub> =C(CH <sub>3</sub> )-COO-(CH <sub>2</sub> ) <sub>6</sub> -O	OCH <sub>3</sub>	H	136	278
M4	CH <sub>2</sub> =C(CH <sub>3</sub> )-COO-(CH <sub>2</sub> ) <sub>6</sub> -O	OC <sub>4</sub> H <sub>9</sub>	H	132	280
M5	CH <sub>2</sub> =C(CH <sub>3</sub> )-COO-(CH <sub>2</sub> ) <sub>2</sub> -O	CN	H	161–164	288

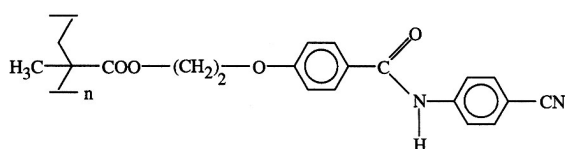
<sup>a</sup> Melting temperature.<sup>b</sup> Absorption maximum.<sup>c</sup> Broad shoulder, starting at nearly 240 nm.

Fig. 2. Homopolymer with para-cyano benzanilide side groups.

tion. Therefore it must be proved that investigations of the photophysical behavior of the benzanilides are not influenced by photochemical deactivation processes [14,15]. The photo-Fries reaction is a 1,3- or 1,5-rearrangement of a molecular fragment at a double bond or at an aromatic system. The radicals formed by homolytical decomposition recombine in the solvent cage by formation of ortho- and para-Fries rearrangement products and by diffusion from the solvent cage by the formation of the corresponding anilines or phenols, respectively (Fig. 3) [16,17].

Figure 4 demonstrates the changes of the absorption properties for the photolysis of benzanilide in cyclohexane. The observed spectral changes follow from the degradation of benzanilide at 266 nm, the formation of *p*-aminobenzophenone at 310 nm and the corresponding ortho-products (*o*-aminobenzophenone) at 360 nm. The solution was irradiated with a wavelength of  $(254 \pm 10)$  nm and an incident capacity of about  $8 \cdot 10^{-4}$  W ml<sup>-1</sup>.

The fluorescence spectra of the benzanilide solution after 60 min of ultraviolet irradiation are shown in Figs. 5a and b. The fluorescence of the *o*-aminobenzophenones excited at 350 nm is little structured and has its maximum at 420 nm (Fig. 5a).

Excitation at 280 nm leads to a very strong fluorescence of the photoproducts, with a maximum at 321 nm, which rapidly overlaps the weak normal fluorescence of benzanilide ( $F_1$ ) at 345 nm (Fig. 5b). Investigations of the para-cyano substituted benzanilide confirm that the fluorescence at 321 nm is not caused exclusively by the photo-Fries products. The shape and

wavelength of the fluorescence maximum suggest that the aniline molecules formed during the photolysis are responsible for the fluorescence at 321 nm [18]. The influence of the photoproducts on the fluorescence spectrum of benzanilide was observed by Azumaya *et al.* [3] and Tang *et al.* [7].

The quantum yield of the photoproduct formation is of the order of  $(1.7 \pm 0.2) \cdot 10^{-3}$  mol einstein<sup>-1</sup> [15]. For the excitation wavelength of 280 nm used for the fluorescence investigations, the quantum yield is only a fifth of the value given in the literature. Moreover, with a value of about  $1 \cdot 10^{-6}$  W ml<sup>-1</sup>, the incident capacity used for the fluorescence measurements is nearly three orders smaller than that used for the investigations of the photochemical behavior of benzanilide. Caused by the excitation at 280 nm, low irradiation intensities, and relatively short measurement times used for the fluorescence investigations, the formation of photo-Fries products can be excluded. In addition, the photoreaction should be hindered in the crystal of the monomers and by the packing of the side groups in the glassy state of the polymers. Furthermore, the wavelength dependence of the photo-Fries reaction prevents the process for irradiation at 350 nm [15,19].

#### Fluorescence Investigations of the Benzanilides and of the Polymer in Solution

The results of the fluorescence investigations of benzanilide (M1) in different solvents are summarized in Table II. Following the solvent, the polarity is expressed by the relative static dielectric constant  $\epsilon_{\text{rel}}$  [20]. The values of the maximum of the fluorescence band [ $\lambda_{\max}(F_2, F_3)$ ] and of the band half-width [bhw( $F_2, F_3$ )] refer to the long-wavelength fluorescence. The fluorescence intensity of the normal fluorescence is very weak and the maximum of the normal fluorescence [ $\lambda_{\max}(F_1) \sim 345$  nm] is independent of the solvent polarity.

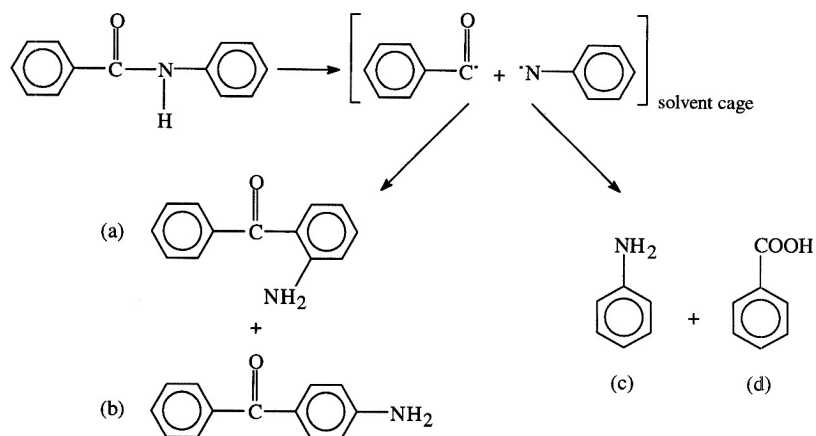


Fig. 3. Formation of (a) *o*- and (b) *p*-aminobenzophenone as well as (c) aniline and (d) benzoic acid by photo-Fries rearrangement of benzanilide.

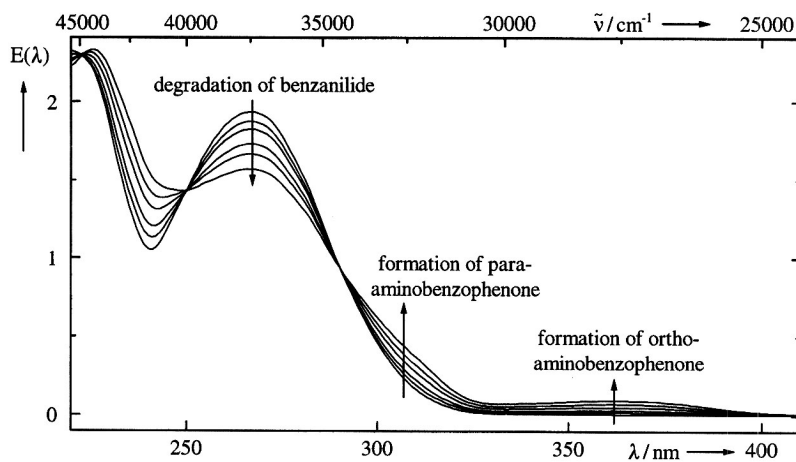


Fig. 4. Changes of the absorption spectrum during the photolysis of benzanilide.

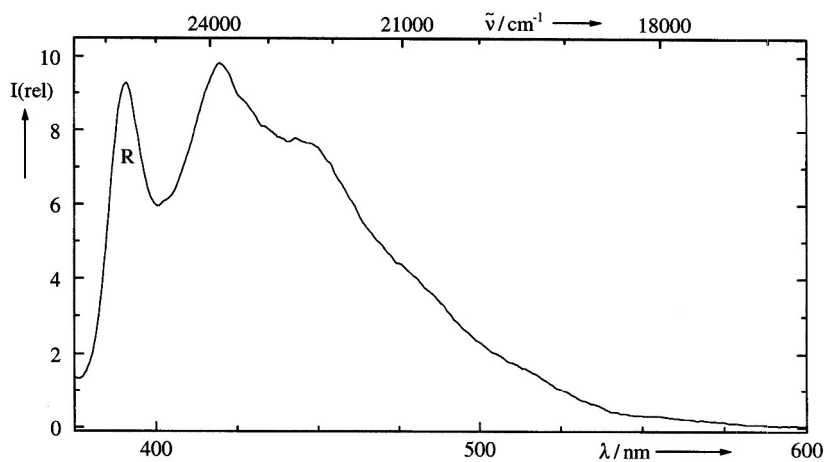


Fig. 5a. Fluorescence of the irradiated solution of benzanilide for excitation at 350 nm (R Raman signal of the solvent).

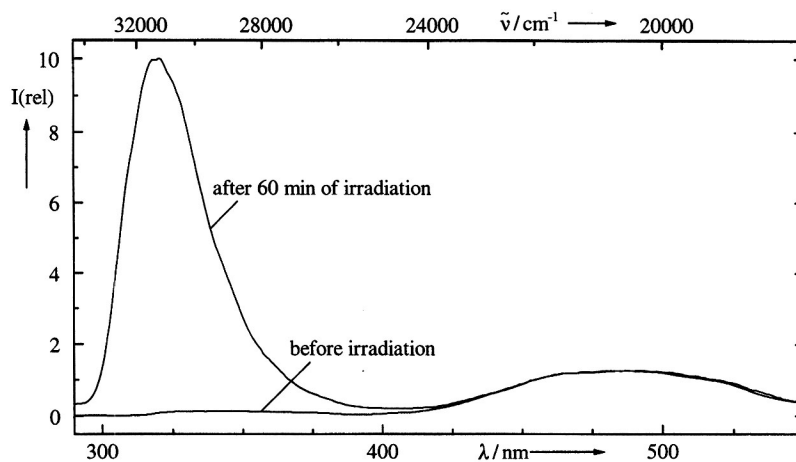


Fig. 5b. Comparison of the fluorescence spectra of benzanilide before and after irradiation with excitation at 280 nm.

Table II. Spectroscopic data on the Fluorescence of M1 in Dependence on the Solvent Polarity

Solvent	$\epsilon_{rel}$	$\lambda_{max}(F_2, F_3)$ (cm <sup>-1</sup> )	bhw (F <sub>2</sub> , F <sub>3</sub> ) (cm <sup>-1</sup> )	$I(F_2, F_3) / I(F_1)^a$
Pentane	1.84	20,660	4,010	8.42
Hexane	1.89	20,620	4,010	9.5
Heptane	1.92	20,660	3,910	10.2
Cyclohexane	2.02	20,620	3,820	10.8
1,4-Dioxane	2.22	19,160	3,240	1.4
Toluene	2.39	19,270	3,210	— <sup>b</sup>
Dibutyl ether	3.14	19,420	3,170	— <sup>b</sup>
Diethyl ether	4.33	19,420	3,120	1.9
Acetic acid <sup>c</sup>	5.4	—	—	—
Ethyl acetate	6.02	19,030	2,670	1.1
Tetrahydrofuran	7.3	19,065	2,850	1.7
Dichloromethane	8.9	18,940	2,950	1.1
Dichloroethane	10.4	18,975	2,700	2.6
Ethanol <sup>c</sup>	25.1	—	—	—

<sup>a</sup>  $I(F_1)$ : fluorescence intensity of the maximum of the short-wavelength band;  $I(F_2, F_3)$ : fluorescence intensity of the maximum of the long-wavelength band.

<sup>b</sup> Strong self-fluorescence of the solvents in the region of the normal benzanilide fluorescence.

<sup>c</sup> Within the bounds of measure precision, no long-wavelength fluorescence noticeable.

In accordance with the results of Heldt and Kasha [1], a variation of the band half-width and a wavelength shift of the band maximum of the long wavelength fluorescence are observed, dependent on the solvent polarity. In nonpolar solvents, like hydrocarbons, the maximum of the long-wavelength fluorescence is at nearly 485 nm and the band half-width is about 4000 cm<sup>-1</sup>. The quantum yield of this fluorescence is of the order of 2.5·10<sup>-3</sup> in these nonpolar solvents. Previous investigations indicated that increasing solvent polarity

leads to a gradual decrease in band half-width. But the experimental data presented in Table II show that only a small increase in the dielectric constant from 2.0 to 2.2 results in a sudden change of the band half-width and of the position of the band maximum. For solvents of higher polarity the maximum of the long-wavelength fluorescence appears at nearly 525 to 528 nm and the band half-width is about 2800 cm<sup>-1</sup>. The quantum yield decreases strongly for polar solvents. It is only 5·10<sup>-4</sup> for the fluorescence of benzanilide in THF. The spectral

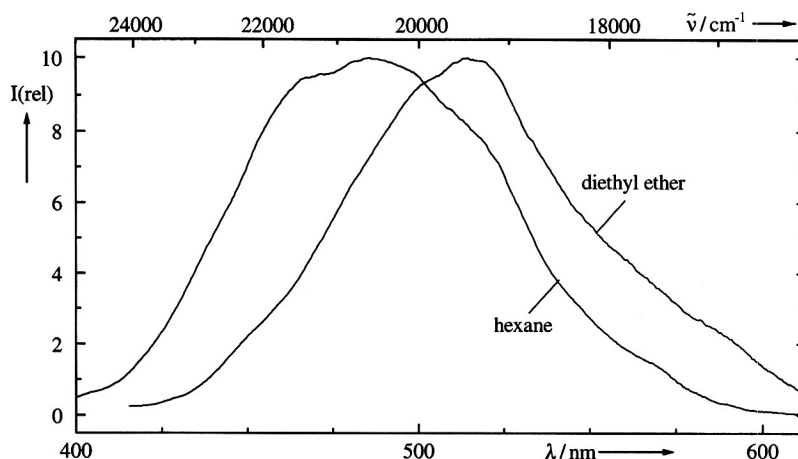


Fig. 6. Long-wavelength fluorescence components of benzanilide in different polar solvents (*n*-hexane and diethyl ether as examples).

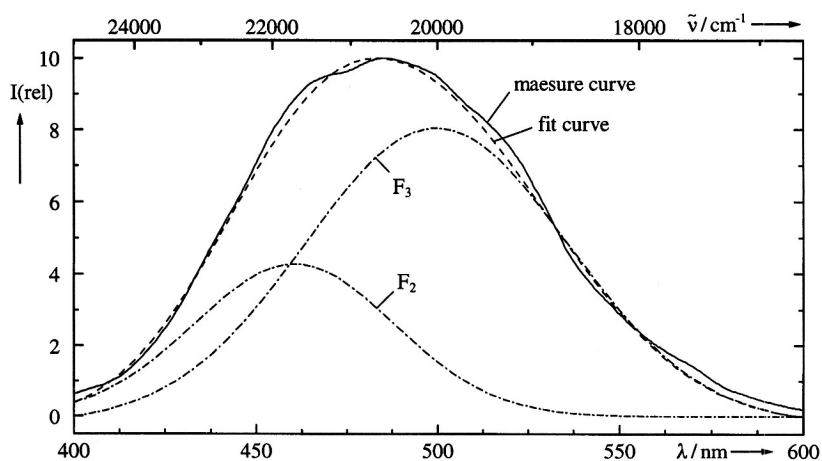


Fig. 7. Band separation of the long-wavelength region of the benzanilide fluorescence (in hexane).

changes caused by increasing solvent polarity are demonstrated in Fig. 6, showing the fluorescence spectra of benzanilide in *n*-hexane and diethyl ether.

The decrease in band half-width as well as the red shift of the band maximum with increasing solvent polarity indicates that, in the case of benzanilide, two long-wavelength fluorescences exist which are influenced sensitively by the solvent. The superposition of the two fluorescences  $F_2$  and  $F_3$  is observed exclusively in hydrocarbon solvents as demonstrated in Fig. 7. While  $F_2$  appears only in hydrocarbon solvents the second long-wavelength fluorescence  $F_3$  is also observed in solvents of higher polarity. The slight bathochromic shift of  $F_3$  with increasing solvent polarity represents the energetic stabilization of the emitting state.

Heldt and Kasha interpret the fluorescence  $F_2$  as proton transfer fluorescence of benzanilide, supposing that this intramolecular proton transfer is formed by *cis* conformers resulting in dimers (concerted biprotonic transfer) [21]. The observed fluorescence  $F_2$  is attributed to the *cis*-imidol tautomer formed by proton transfer. However, investigations of the ground-state structure of benzanilide give no evidence for a *cis* conformation of the molecules.

Whereas X-ray and NMR measurements suggest that the amide group of benzanilide in the ground state exists in the *trans* conformation not only in the crystal but also in solution and as an isolated molecule in vacuum [22,23], *N*-methylbenzanilide generally appears in the *cis* conformation. The *trans* conformation of benzan-

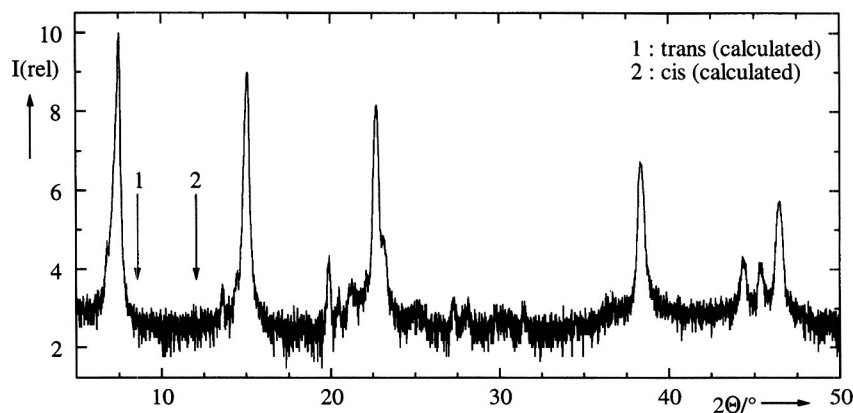


Fig. 8. X-ray diagram of the benzanilide crystal.

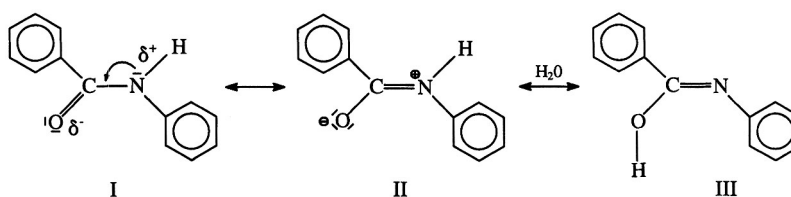


Fig. 9. Formation of the imidol structure of benzanilide by resonance.

ilide is confirmed by our own X-ray measurements (Fig. 8). From the signal at  $2\Theta = 7.5^\circ$  an extension of the benzanilide molecule of  $11.7 \text{ \AA}$  can be determined. Molecular calculations (computer program Alchemie 3.0) of the extension of benzanilide result in a value of  $7.4 \text{ \AA}$  for the *cis* conformation and of  $10.2 \text{ \AA}$  for the *trans* conformation. The calculation is based on the assumption that the molecules are in the gas phase. Therefore the value determined from the diagram is in good agreement with the calculated value for the *trans* conformation. In the region where a peak for the *cis* conformation has to be expected ( $2\Theta \sim 12.0^\circ$ ), no signal is observed.

Further evidence for the *trans* structure of the molecules is given by IR investigations of benzanilide in KBr as well as by the FTIR spectrum of the benzanilide crystal. The position of the N–H valence band at  $3345 \text{ cm}^{-1}$  given in the literature [24] with  $3300 \text{ cm}^{-1}$  points to the existence of associated *trans* molecules. For molecules in the *cis* conformation a signal at nearly  $3160 \text{ cm}^{-1}$  should be expected. Because at present there is no evidence that an aggregation of *cis*-benzanilide molecules is responsible for the PT fluorescence, other reasons for the proton transfer should be discussed. One possible reason for the observed proton transfer is the aggregation of *trans*-benzanilides. The concentration independence of the PT fluorescence suggests that an ag-

gregation process also occurs for concentrations of about  $10^{-5} \text{ M}$  in hydrocarbons. Obviously the interaction between the benzanilide molecules should be favorable compared to benzanilide–hydrogen interaction.

Nevertheless, it cannot be excluded that a monomolecular process is responsible for the PT mechanism. The imidol structure of benzanilide can also be formed because of the resonance of the amid bond if it is presumed that, in the hydrocarbon solvents, a few water molecules with promoting influence exist (Fig. 9).

Further evidence of the superposition of PT and ICT fluorescence in nonpolar solvents has been found by the addition of a small amount of ethanol (up to 1.5% of the solution) to a solution of benzanilide in *n*-hexane.

Figure 10 shows that an increase in ethanol leads to a drastic decrease in fluorescence intensity and to a red shift of the band maximum of about 20 nm. The formation of intermolecular hydrogen bonds between the alcohol and the amide group restricts the formation of hydrogen bonds between the benzanilide molecules respectively the formation of the polar resonance structure. As a consequence, strong quenching of the PT fluorescence occurs, while the ICT fluorescence, which is less influenced by the small amount of ethanol, is still observed.

On the basis of the same argument, it can be explained that no long-wavelength fluorescence has been

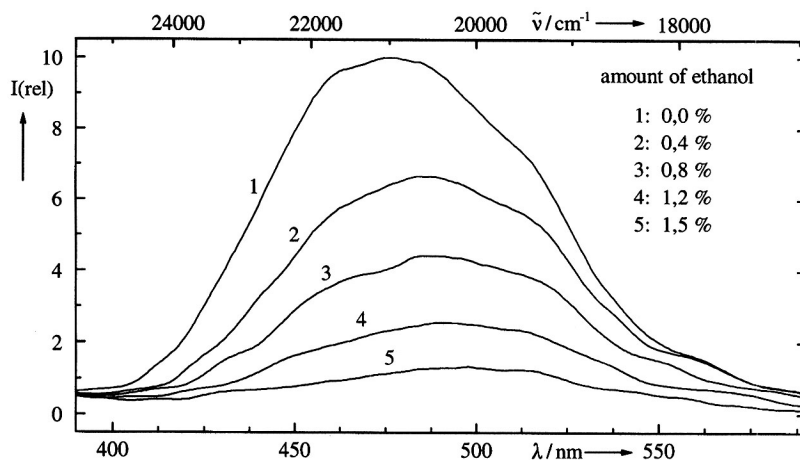


Fig. 10. Change of the fluorescence behavior by on the addition of ethanol to a  $10^{-4}$  M solution of benzanilide (**M1**) in *n*-hexane.

Table III. Spectroscopic Data on the Fluorescence of **M2** in Dependence on the Solvent Polarity

Solvent	$\epsilon_{\text{rel}}$	$\lambda_{\text{max}} (F_2, F_3)$ (nm)	bhw ( $F_2, F_3$ ) ( $\text{cm}^{-1}$ )	$I(F_2, F_3) / I(F_1)$
Pentane	1.84	19,230	2,910	12.4
Hexane	1.89	19,175	2,970	5.6
Heptane	1.92	19,160	2,950	6.9
Cyclohexane	2.02	19,160	2,950	8.8
1,4-Dioxane	2.22	18,835	— <sup>a</sup>	0.08
Toluene	2.39	18,870	3,240	— <sup>b</sup>
Dibutyl ether	3.14	18,940	3,240	0.07
Diethyl ether	4.33	18,955	— <sup>a</sup>	— <sup>b</sup>
Acetic acid <sup>c</sup>	5.4	—	—	—
Tetrahydrofuran	7.3	18,760	— <sup>a</sup>	< 0.05

<sup>a</sup> Band half-width not determinable because of low intensities.  $I(F_2, F_3)$ : fluorescence intensity of the maximum of the long-wavelength band.

<sup>b</sup> Strong self-fluorescence of the solvents in the region of the normal benzanilide fluorescence.

<sup>c</sup> Within the bounds of measure precision, no long-wavelength fluorescence noticeable.

observed in protic solvents (acetic acid, ethanol). As mentioned above, a strong interaction between benzanilide and solvent molecules occurs in the form of hydrogen bonds, leading to a quenching of the PT fluorescence. Moreover, it is known that the quantum yield of amino compounds is strongly quenched in protic solvents [10] so that the weak ICT fluorescence is also no longer observed.

The decrease in band half-width by the change from hydrocarbon solvents to more polar solvents as well as the constancy of the half-width with further increase of the dielectric constant suggests that there is only one emitting species responsible for the fluorescence behavior with  $\epsilon_{\text{rel}} \geq 3$ . The observed red shift of the band maximum representing an energetical stabilization of the emitting state supports the hypothesis of Azumaya *et al.* and Heldt *et al.* that an ICT/TICT state is responsible

for the second long-wavelength fluorescence  $F_3$ . But in contradiction to classical ICT/TICT systems, where donor and acceptor are connected via a benzene ring, in the case of benzanilide the amino donor group and carbonyl acceptor group are placed side by side.

However, the investigation of 4-methoxy-*N*-methylbenzanilide (**M2**) verifies that one of the long-wavelength fluorescences can actually be recognized as a proton transfer fluorescence. The results of the solvent dependence of **M2** are given in Table III.

In addition to the normal fluorescence at 335 nm a long-wavelength fluorescence is observed in the case of **M2**, too. In contradiction with the long-wavelength fluorescence of benzanilide, the band half-width of the fluorescence of **M2** is nearly the same in all solvents used. With a value of  $2900 \text{ cm}^{-1}$ , it is in good agreement with the half-width of the **M1** fluorescence in polar solvents.



The constancy of the half-width indicates that only one emitting species is responsible for the long-wavelength band of the **M2** fluorescence. Because the methylation prevents a proton transfer process, the long-wavelength fluorescence of **M2** can be interpreted as ICT fluorescence. This is supported by the bathochromic shift of this fluorescence with increasing solvent polarity. This shift is of the order of  $470\text{ cm}^{-1}$  and is smaller than the shift of the benzanilide fluorescence of  $1680\text{ cm}^{-1}$ . The bathochromic shift of the fluorescence of 4-methoxy-*N*-methylbenzanilide represents the energetical stabilization of the emitting state, but in the case of benzanilide the quenching of the PT fluorescence additionally affects the position of the band maximum.

Although the shift of the long-wavelength fluorescence band of benzanilide and 4-methoxy-*N*-methylbenzanilide points to the existence of an ICT or TICT process as discussed by Azumaya and Heldt, the deactivation processes of benzanilide seem to be more complicated. So the observed shift of nearly  $470\text{ cm}^{-1}$  of  $F_3$  is relatively small compared with classical ICT/TICT systems. Moreover, it is remarkable that the ratio of the maximal intensities of long- and short-wavelength fluorescence  $I(F_2, F_3)/I(F_1)$  decreases strongly with the increase in the solvent polarity for **M1** as well as for **M2**. This result is in contradiction to the expectation that the energetical stabilization of the emitting state results in both a bathochromic shift of the spectrum and a relative growth of the intensity of the ICT fluorescence compared with the normal fluorescence. However, the observations suggest that the emitting state responsible for the short-wavelength fluorescence is more polar than the long-wavelength emitting state. Because this result is characteristic for the fluorescence of both **M1** and **M2**, it cannot be caused by the quenching of the PT fluorescence.

The observations become more clear if the specific properties of the CONH peptide bond are discussed. Already in the ground state there exists a resonance so that the amino group undergoes partial  $sp^2$ -hybridization by formation of a double bond between the nitrogen and the carbon atom of the carbonyl group. The resonance structures of benzanilide are shown in Fig. 9 (**I**, **II**).

Investigations of polyenes [25,26] as well as analogous considerations of the solvent dependence of keto-enol equilibria [27] suggest that an increase in the solvent polarity results in a shift of the relation of the resonance structures to the more polar resonance structure **II**. The corresponding increase in the partial double-bond character leads to a stabilization of the planar form of benzanilide, whereas changes like rotation about the C-N bond or the amino nitrogen inversion are probably strongly hindered. So it becomes understandable that

with an increase in solvent polarity, a preference of the normal  $F_1$  fluorescence of the planar benzanilide molecule is observed.

Furthermore, the comparison of the fluorescence properties of **M1** and **M2** shows that, for identical environmental conditions, the maximum ICT fluorescence of **M2** appears at longer wavelengths than that of **M1**. As for **M2**, the methyl group leads to an increase in the electron density at the nitrogen atom, resulting in a more suitable charge distribution for the ICT process than in the case of **M1**.

Moreover, the determination of the ratio of the maximal intensities of long- and short-wavelength fluorescence  $[I(F_2, F_3)/I(F_1)]$  results in lower values for **M2** than for **M1** provided by the same solvent (with the exception of pentane). Obviously the higher electron density at the nitrogen atom of **M2** corresponds with an increase in the partial double-bond character of the C-N bond, resulting in a stabilization of the planar form of the molecules. That seems to be the reason for the higher portion of normal fluorescence in the spectrum of **M2** compared with **M1**.

To support the PT/ICT hypothesis, the benzanilide molecules **M3**, **M4**, and **M5**, whose different para-substitutions modify the electron density at the nitrogen atom, were investigated. It has to be expected that the alkoxy groups, as electron donors, increase the electron density, while the cyano group, as the electron acceptor, decreases it.

In Fig. 11 the fluorescence spectra of the cyano substituted benzanilide (**M5**) in different polar solvents are shown. The corresponding experimental data are presented in Table IV. In addition to a relatively strong normal fluorescence, the long-wavelength fluorescence is observed, with its maximum at 432 nm in hydrocarbon solvents. The band half-width of the long-wavelength fluorescence is in the region of  $5200$  to  $5500\text{ cm}^{-1}$  in cyclohexane. It can be proved that this fluorescence is essentially characterized by the PT fluorescence because the cyano substitution of **M5** leads to a charge distribution unsuitable for the ICT mechanism. Compared with benzanilide, the acceptor property at the carbon atom of the amide group is weakened by the donor property of the alkoxy fragment. In addition, the electron density at the nitrogen atom is reduced by the acceptor property of the cyano group.

As shown in Table IV the half-width of the long wavelength fluorescence is relatively constant for all used solvents with higher polarity. In this region of polarity the ICT fluorescence is responsible for the long-wavelength fluorescence. The restriction of the ICT mechanism by the cyano substitution is especially re-

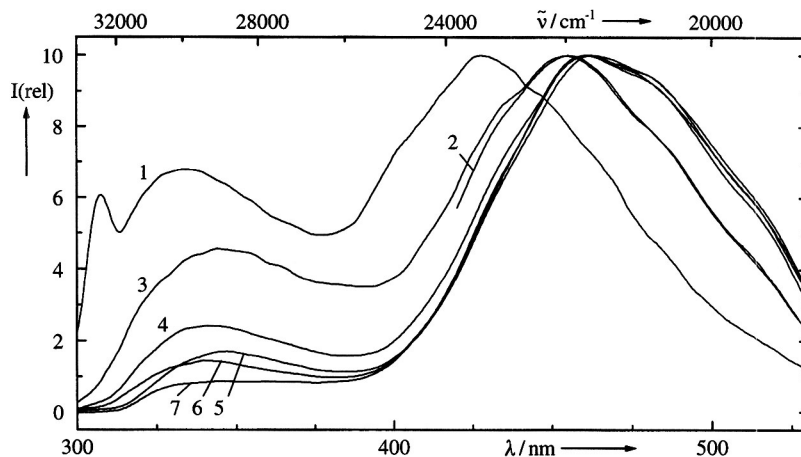


Fig. 11. Fluorescence spectra of the cyano substituted benzanilide monomer in different polar solvents 1, Cyclohexane; 2, toluene; 3, dibutyl ether; 4, diethyl ether; 5, tetrahydrofuran; 6, dichloromethane; 7, dichloroethane.

Table IV. Spectroscopic data on the Fluorescence of **M5** in Dependence on the Solvent Polarity

Solvent	$\epsilon_{\text{rel}}$	$\lambda_{\text{max}} (F_2, F_3) \text{ (nm)}$	bhw ( $F_2, F_3$ ) ( $\text{cm}^{-1}$ )	$I(F_2, F_3) / I(F_1)$
Cyclohexane	2.02	23,120	5,200–5,500	— <sup>a</sup>
Toluene	2.39	21,690	4,467	— <sup>a</sup>
Dibutyl ether	3.14	21,740	4,780	1.52
Diethyl ether	4.33	21,550	4,560	2.94
Ethyl acetate	6.02	21,460	4,410	5.4
Tetrahydrofuran	7.3	21,505	4,400	4.6
Dichloromethane	8.9	21,480	4,390	5.03
Dichloroethane	10.4	21,505	4,360	8.33

<sup>a</sup> Strong self-fluorescence of the solvents in the region of the normal benzanilide fluorescence.

flected in the position of the band maximum. Under comparable conditions the maximum of the ICT band of **M5** appears at a shorter wavelength than that of the **M1** ICT band. Differences up to 50 nm respectively 2500  $\text{cm}^{-1}$  can be found by comparison of the values in Tables II and IV.

In the case of **M5** the competition between normal fluorescence and ICT fluorescence can be demonstrated in dependence on the solvent polarity. The spectra in Fig. 11 show that the intensity of the normal short-wavelength fluorescence decreases in comparison with the intensity of the long-wavelength fluorescence with increasing solvent polarity. This process is represented in Table IV in the relation of the intensities of the maxima of long-wavelength and short-wavelength fluorescence [ $I(F_2, F_3)/I(F_1)$ ]. In addition to an increase in the relative intensity of the ICT fluorescence with increasing environmental polarity, a bathochromic shift of the band is observed, indicating the stabilization of the ICT state.

This process occurs suddenly for a range of dielectric constant between  $\epsilon_{\text{rel}} = 3.14$  and  $\epsilon_{\text{rel}} = 4.33$ . Above this range no change in the band position appears. Because this behavior, which is typical for ICT fluorescences, has not been found for benzanilide and 4-methoxy-*N*-methylbenzanilide, it can be assumed that in the case of the cyano substituted monomer, a different ICT process dominates the fluorescence behavior. While the charge transfer of benzanilide occurs between the amino nitrogen atom and the adjacent carbon atom in the case of **M5** because of the cyano substitution, a charge transfer between the amino nitrogen and the benzonitrile group is imaginable as discussed in the case of aminobenzonitriles [28] (Fig. 12).

Because the substitution patterns of **M3** and **M4** scarcely differ in solution, no significance of the fluorescence behavior of the monomers has been found. Both monomers show a distinctive long-wavelength fluorescence in hydrocarbon solvents. The maximum of

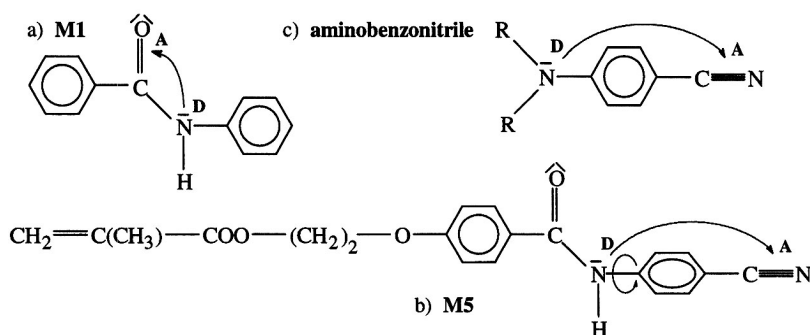


Fig. 12. Possibilities for the charge transfer in (a) benzanilide, (b) cyano substituted benzanilide, and (c) aminobenzonitrile.

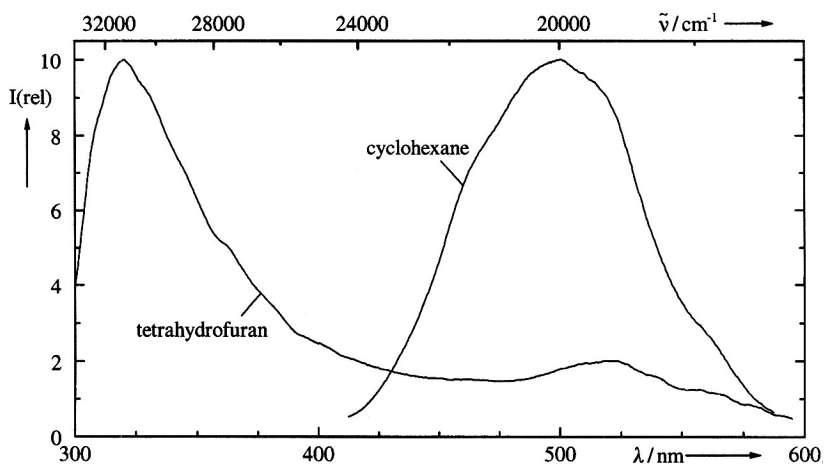


Fig. 13. Comparison of the fluorescences of M3 in cyclohexane and tetrahydrofuran.

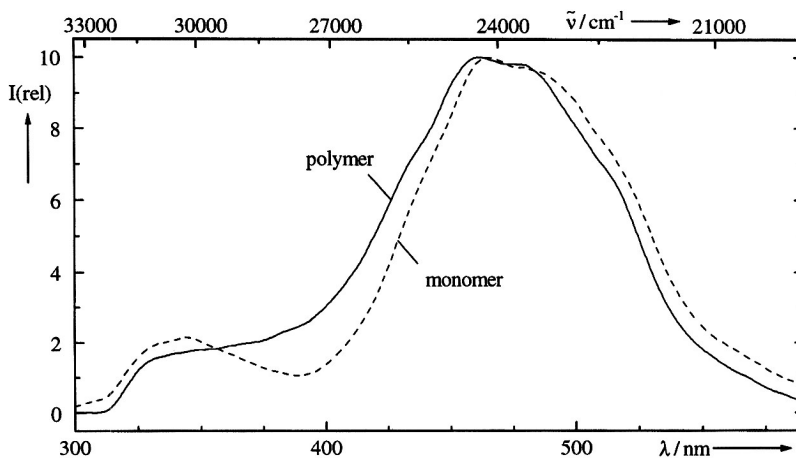


Fig. 14. Comparison of the fluorescence spectra of the cyano- substituted monomer and polymer in tetrahydrofuran.

this fluorescence appears at nearly 499 nm and the band half-width is about  $3600\text{ cm}^{-1}$  (Fig. 13). The fluorescence intensity of **M3** and **M4** is extremely weak in polar solvents. However, the spectra in Fig. 13 show that the band maximum shifts to a higher wavelength [ $\lambda_{\text{max}}(\text{F}_3) \sim 521\text{ nm}$ ] because of the promotion of the ICT state and the restriction of the proton transfer.

Corresponding to the fluorescence behavior of the benzanilide monomers, the investigation of polymers with benzanilide side groups shows that, in addition to the normal fluorescence, the characteristic long-wavelength fluorescence of benzanilide is observed (Fig. 14).

In accordance with the monomer fluorescence of **M5**, the maximum of the long-wavelength fluorescence of polymer **P5** appears at 465 nm. The band half-width of the polymer fluorescence of  $4860\text{ cm}^{-1}$  is somewhat higher than that of the monomer fluorescence. Moreover, the short-wavelength and long-wavelength bands of the polymer fluorescence are less separated than the corresponding monomer bands. The long-wavelength band of the polymer fluorescence can be interpreted as ICT fluorescence because the high polarity of the solvent used disturbs the proton transfer. Because of the poor solubility of the polymers and the high local concentrations within the polymer coil, intermolecular processes, like excimer formation, cannot be excluded, which could cause the observed small differences between monomer and polymer fluorescence. But overall, the fluorescence of the polymer corresponds quite well to that of the monomer.

### Fluorescence of the Crystalline Benzanilide Monomers

Figure 15 shows the fluorescence spectra of the crystalline benzanilide monomers **M1** and **M2**. Corresponding to the investigations in solution, the maximum of the long-wavelength fluorescence band of **M1** at 440 nm appears at a lower wavelength than that of **M2** at 524 nm.

Because of the crystallinity of the benzanilide monomers and the corresponding strong tendency to the formation of intermolecular hydrogen bonds, it can be presumed that the observed long-wavelength fluorescence of **M1** is essentially caused by the PT mechanism. However, it is astonishing that a long-wavelength fluorescence is found for the crystalline 4-methoxy-*N*-methylbenzanilide, too. Because the methylation of **M2** prevents the PT fluorescence, the results suggest that there is also enough free volume for the ICT mechanism in the solid state of the monomers. Investigations of other TICT systems show that the twisting process is

strongly restricted in rigid solutions and crystalline systems, caused by the lack of free volume [29]. The changes in the conformation of the molecules resulting from the amino nitrogen inversion require less free volume compared with a rotation process of the molecules. So the surprising observation of an ICT fluorescence of the crystalline benzanilides suggests that the intramolecular charge transfer corresponds to a planarization of the molecules and an increase in the partial double-bond character of the C–N bond.

It can be presumed that the portion of ICT fluorescence in the long-wavelength fluorescence is relatively small. Nevertheless, corresponding to the investigations in solution, the dependence of the benzanilide fluorescence from the para-substitution is reflected in the spectra of the crystalline substances, too. For illustration, the spectra of **M3** and **M5** are shown in Fig. 16.

It is found that the fluorescence maximum of the cyano substituted monomer [ $\lambda_{\text{max}}(\text{F}_2, \text{F}_3) = 485\text{ nm}$ ] appears at a shorter wavelength than that of the methoxy substituted one [ $\lambda_{\text{max}}(\text{F}_2, \text{F}_3) = 502\text{ nm}$ ]. Moreover, the band half-width of the fluorescence of **M5** is smaller than that of the **M3** fluorescence. The long-wavelength fluorescence of **M5** is characterized mainly by the PT fluorescence because the cyano substitution results in adverse prerequisites for the ICT mechanism. Compared with the cyano substitution, the methoxy substitution leads to a suitable electron distribution for the ICT mechanism, resulting in an increase in the band half-width as well as a small red shift of the band maximum.

Comparison investigations of the deactivation behavior of the crystalline monomers and solid polymers show that the fluorescence maximum of the long-wavelength fluorescence of the polymers [**P5**:  $\lambda_{\text{max}}(\text{F}_2, \text{F}_3) = 500\text{ nm}$ ] appears at a longer wavelength than that of the corresponding monomers [**M5**:  $\lambda_{\text{max}}(\text{F}_2, \text{F}_3) = 485\text{ nm}$ ]. Moreover, the band half-width of the polymer fluorescence is higher than that of the monomer fluorescence. A possible explanation for these differences is that because of the crystallinity of the monomers, suitable prerequisites for the formation of hydrogen bonds are given, whereas in the less-ordered polymer glass, better conditions exist for the ICT mechanism [30].

### CONCLUSIONS

The photophysical deactivation behavior of benzanilide is characterized by three competitive processes. Because of the strong influence of the specific of the amide bond (resonance, capability for the formation of hydrogen bonds), the emission behavior of benzanilide in so-

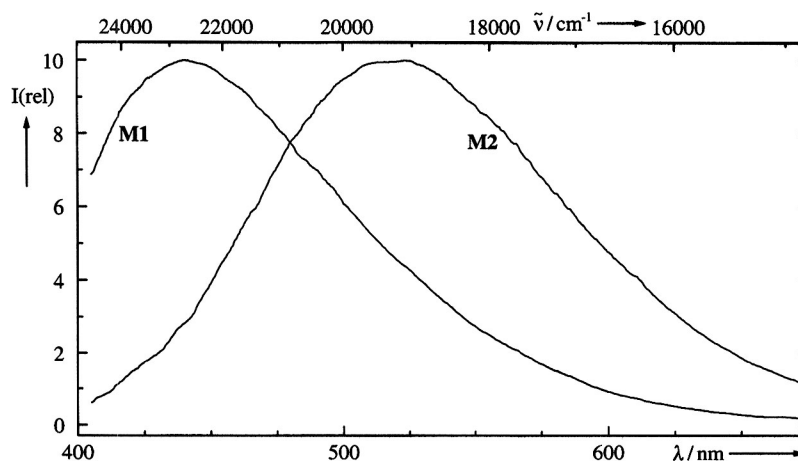


Fig. 15. Fluorescence of the crystalline benzanilides M1 and M2.

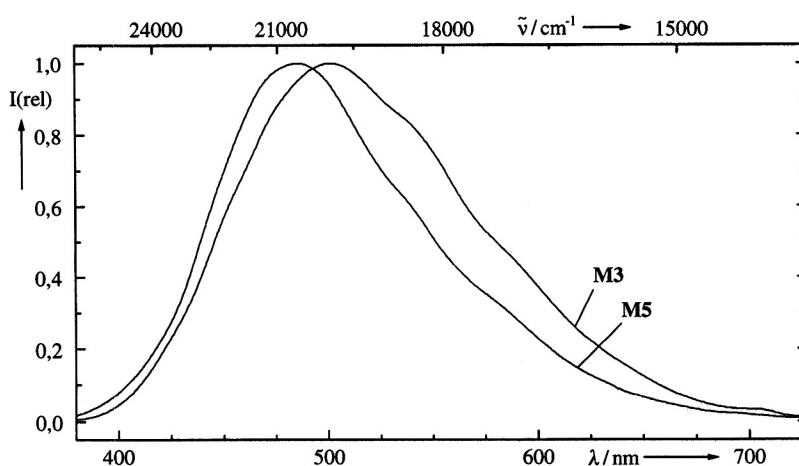


Fig. 16. Fluorescence behavior of the crystalline monomers in dependence on the para-substitution.

lution largely agrees with the behavior of the crystalline monomers and those of the polymers in the solid state. An influence of the photo-Fries reaction of benzanilide has been carefully excluded under the experimental conditions of the fluorescence measurements.

The normal fluorescence of benzanilide is very weak and has its maximum at 345 nm. Corresponding to the investigations by Heldt and Kasha [1], it was possible to characterize the broad Stokes-shifted fluorescence in the wavelength region of 480 to 520 nm as a superposition of two fluorescences because of its sensitivity to environmental conditions. This conclusion is based on the following experimental results.

1. With an increase in solvent polarity, a red shift of the maximum of the long-wavelength fluo-

rescence band as well as a decrease in the band half-width is observed.

2. There is no change in the band half-width observed for 4-methoxy-*N*-methylbenzanilide in dependence on the solvent polarity. The band half-width of 4-methoxy-*N*-methylbenzanilide is of the order of the band half-width of the benzanilide fluorescence in polar solvents.

These results are in contrast to the interpretation of Azumaya *et al.* [3] that there is only one emitting species responsible for the long-wavelength fluorescence of benzanilide and 4-methoxy-*N*-methylbenzanilide.

The comparison of the fluorescence spectra of benzanilide and 4-methoxy-*N*-methylbenzanilide as well as the investigation of the influence of protic solvents on

the fluorescence behavior of benzanilide indicates that the long-wavelength fluorescence with the shorter maximum ( $F_2$ ) is caused by an intermolecular proton transfer between trans isomers, which exist as aggregates in non-polar solvents.

The second long-wavelength fluorescence ( $F_3$ ) of benzanilide can be interpreted as ICT fluorescence because of its dependence on the solvent polarity as well as on the para-substitution. Because the ICT fluorescence is observed not only in solution but also for the crystalline monomers, a twisting of the molecules as proposed by Heldt *et al.* and Azumaya *et al.* is improbable. The results can be explained by the model of the amino nitrogen inversion, according to which the intramolecular charge transfer of benzanilide corresponds with an increase in the partial double-bond character of the amide bond and a planarisation of the molecules.

An investigation of the fluorescence behavior of amorphous and liquid crystalline polymethacrylates with benzanilide side groups in dependence on the temperature in relation to their thermotropic properties as well as fluorescence investigations of corresponding spin-coated polymer films is in preparation.

## ACKNOWLEDGMENTS

The authors thank Dr. R. Ruhmann, Institute of Advanced Chemistry Berlin Adlershof e.V., for the preparation of the investigated monomers and polymers. Furthermore, thanks are due to Dr. T. Geue for the x-ray measurements and to Dr. H. Schmidt for stimulating discussions (both at the University of Potsdam).

## REFERENCES

- J. Heldt and M. Kasha (1989) *J. Mol. Liquids* **41**, 305–313.
- E. J. O'Connell and M. Delmauro (1971) *J. Irwin Photochem. Photobiol.* **14**, 189–195.
- I. Azumaya, H. Kagechika, Y. Fujiwara, M. Itoh, K. Yamaguchi, and K. Shudo (1991) *J. Am. Chem. Soc.* **113**, 2833–2838.
- J. Heldt, D. Gormin, and M. Kasha (1989) *Chem. Phys.* **136**, 321–334.
- J. Heldt, D. Gormin, and M. Kasha (1988) *Chem. Phys. Lett.* **150**(5), 433–436.
- J. Heldt, D. Gormin, and M. Kasha (1988) *J. Am. Chem. Soc.* **110**, 8255–8256.
- G.-Q. Tang, J. MacInnis, and M. Kasha (1987) *J. Am. Chem. Soc.* **109**, 2531.
- Z. R. Grabowski, K. Rotkiewicz, A. Siemiarzczuk, D. J. Cowley, and W. Baumann (1979) *Nouv. J. Chim.* **3**, 443.
- E. Lippert, W. Lüder, and H. Boos (1962) in A. Mangini (Ed.), *Advances in Molecular Spectroscopy*, Pergamon Press, Oxford, p. 443.
- W. Rettig (1986) *Angew. Chem.* **98**, 969–985.
- K. A. Zachariasse, M. Grobys, Th. von der Haar, A. Hebecker, Y. Il'ichev, and W. Kühnle (1996) *J. Inf. Rec.* **22**, 553–560.
- Th. von der Haar, A. Hebecker, Y. Il'ichev, Y.-B. Jiang, W. Kühnle, and K. A. Zachariasse (1995) *Recl. Trav. Chim. Pays-Bas* **114**, 430–442.
- L. Läscher, Th. Fischer, M. Rutloh, S. Kostromin, and R. Ruhmann (1996) *Thin Solid Films* **284**(85), 252–256.
- J. Stumpe, A. Mehlhorn, and K. Schwetlick (1978) *J. Photochem.* **8**, 1.
- D. J. Carlsson, L. H. Gan, and D. M. Wiles (1975) *Can. J. Chem.* **53**, 2337–2344.
- R. Chenevert and R. Plante (1983) *Can. J. Chem.* **61**, 1092–1095.
- A. Itai, Y. Toriumi, N. Tomioka, H. Kagechika, I. Azumaya, and K. Shudo (1989) *Tetrahedron Lett.* **30**(45), 6177.
- I. B. Berlman (1971) *Handbook of Fluorescence Spectroscopy of Aromatic Molecules*, New York.
- S. Singh, D. Creed, and C. E. Hoyle (1992) *Proc. SPIE* **1774**, 2.
- D. R. Lide (1993/1994) *Handbook of Chemistry and Physics*, CRC Press, Boca Raton, FL.
- M. Kasha (1986) *J. Chem. Soc. Faraday Trans.* **82**, 2379–2392.
- I. Azumaya, H. Kagechiká, K. Yamaguchi, and K. Shudo (1995) *Tetrahedron* **51**(18), 5277–5290.
- A. Itai, Y. Toriumi, N. Tomioka, H. Kagechika, I. Azumaya, and K. Shudo (1989) *Tetrahedron Lett.* **30**(45), 6177–6180.
- H. Günzler and H. Böck (1990) *IR-Spektroskopie*, Verlag Chemie GmbH, Weinheim.
- G. Bourhill, J.-L. Bredas, L.-T. Cheng, S. R. Marder, F. Meyers, J. W. Perry, and B. G. Tiemann (1994) *J. Am. Chem. Soc.* **116**, 2619–2620.
- S. R. Marder, C. B. Gorman, F. Meyers, J. W. Perry, G. Bourhill, J.-L. Bredas, and B. M. Pierce (1994) *Science* **265**, 632–635.
- Chr. Reichardt (1973) *Lösungsmittel-Effekte in der organischen Chemie*, Verlag Chemie GmbH, Weinheim.
- K. Rotkiewicz, J. Herbich, F. Perez Salgado, and W. Rettig (1992) *Proc. Ind. Acad. Sci. (Chem. Sci.)* **104**(2), 105.
- J. Herbich, J. Dobkowski, C. Rulliere, and J. Nowacki (1989) *J. Luminesc.* **44**, 87.
- S. Pade, H. Schmidt, J. Stumpe, and Th. Fischer (1996) *J. Inf. Record.* **23**, 117.